JOURNAL OF GEOPHYSICAL RESEARCH, VOL. 104, NO. C4, PAGES 7743–7752, APRIL 15, 1999

Caribbean Sea eddies inferred from TOPEX/POSEIDON altimetry and a 1/6° Atlantic Ocean model simulation

James A. Carton
Department of Meteorology, University of Maryland at College Park

Yi Chao
Jet Propulsion Laboratory, California Institute of Technology, Pasadena

Abstract. Large cyclonic and anticyclonic eddies are found in the Caribbean Sea. Analysis of sea level data from the TOPEX/POSEIDON altimeter shows that the eddies are quite regular, appearing at near 3-month intervals west of the southern Lesser Antilles. These eddies progress westward at average speeds of 12 cm s^{-1}, growing in amplitude up to 20 cm. Many eddies dissipate in the coastal waters of Nicaragua a half year after they appear. A 1/6° × 1/6° general circulation model of the Atlantic is shown to reproduce major features of the eddy life cycle, including their amplitudes, temporal scales, and propagation speed. Analysis of the model output further suggests that the eddies are mainly limited to the thermocline and above, with little phase lag in the vertical. The simulated eddies have sufficiently strong currents that the horizontal gradient of total vorticity changes sign, suggesting that conversions from mean to eddy kinetic energy may be contributing to their growth. Analysis of the simulation links eddies in the Caribbean with eddies formed outside the Caribbean at the confluence of the North Brazil Current and North Equatorial Countercurrent systems.

1. Introduction

The Caribbean Sea, a deep, semienclosed basin, plays an important role in closing the mass budget of the Atlantic Ocean. The mean currents of the southern Caribbean are dominated by the strong westward Caribbean Current that flows into the basin through the islands of the southern Lesser Antilles (Figure 1). This current sweeps past the Yucatan peninsula and continues into the Gulf of Mexico [*Wust*, 1964; *Gordon*, 1967], exiting through the Florida Straits at a rate of 30×10^6 m^3 s^{-1} [*Schmitz and Richardson*, 1991]. Its speed in the southern Caribbean may average 60 cm s^{-1} [*Molinari et al*., 1981].

Roughly half of the transport in this current enters the southern Caribbean through the narrow Grenada, Saint Vincent, and Saint Lucia Passages of the southern Lesser Antilles [see *Mazeika et al*., 1983; *Kinder et al*., 1985, and references therein]. Water coming through the Windward Islands is generally assumed to originate in the Southern Hemisphere, transported there by variable currents along the eastern boundary of South America [*Schmitz and Richardson*, 1991]. A few channels are deep enough to admit water to depths of 900 m. Other than these narrow channels most of the transport into the Caribbean occurs at depths shallower than 200 m. The shallowness of these latter passages ensures that the Caribbean Current has a shallow vertical structure and strong vertical shear in the east.

The Caribbean Sea is also known to have pronounced variability in both space and time. The sea level record at La Guaira in central Venezuela is shown in Figure 2. This port is exposed to the Caribbean Sea with only a 20-km continental shelf. The most energetic signals in the record are quasi-periodic, 20-cm peak-to-peak fluctuations with timescales of near a 3-month period. We believe the cause of these sea level fluctuations is the westward passing of large-amplitude mesoscale eddies. Such eddies also seem apparent in a hydrographic survey by the Colombian Navy in 1975, shown in Figure 3. The presence of strong eddy variability in this region may explain why *Gordon* [1967] observed counterclockwise circulation in the southwestern Gulf de Los Mosquitos, then *Molinari et al*. [1981] observed clockwise circulation, while *Kinder et al*. [1985] found counterclockwise circulation had returned. The sources and evolution of eddies in the southern Caribbean Sea are the main topics of this paper.

The first published evidence of eddy activity in the southern Caribbean was the discovery of two eddies to the west of the Lesser Antilles by *Ingham and Mahnken* [1966]. These eddies were confined mainly above 150 m, with maximum surface currents of 1 m s^{-1}. In a reexamination of the data, *Leming* [1971] proposed that the eddies were part of an island wake resulting from flow past the Lesser Antilles. A comprehensive documentation of the eddy field came from deployments of 23 drifters during the fall and winter seasons of 1975–1977 [*Molinari et al*., 1981; *Heburn et al*., 1982; *Kinder*, 1983]. The drifter tracks showed evidence of eddy activity throughout the southern Caribbean; but the distribution of observations led the authors to assume that the eddy activity occurred mainly in the eastern basin. Successive drifters that seemed to measure the same eddy implied westward propagation with speeds of 10 cm s^{-1}. *Molinari et al*. [1981] suggested that the appearance of eddies near the Aves Swell was the result of interaction between the mean flow and the topography. A different generation mechanism was proposed by *Heburn et al*. [1982] using a two-layer model, suggesting that the eddies result from barotropic instability of the strong currents flowing through the Lesser Antilles.

Paper number 1998JC900081.
0148-0227/99/1998JC900081$09.00

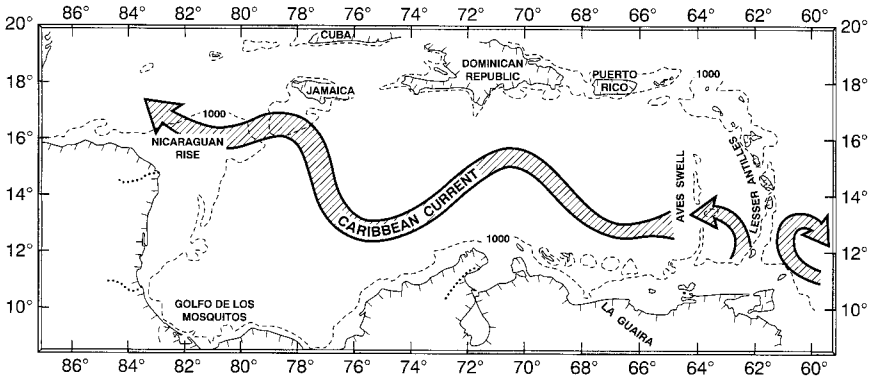

Figure 1. Basin geometry. Dashed line shows 1000-m isobath. Instantaneous path of the Caribbean Current is sketched.

Because of their sparse distribution, the drifters were unable to resolve the space or timescales of the eddies. Synthetic aperture radar measurements from Seasat [*Fu and Holt*, 1983] and altimetry from Geosat [*Nystuen and Andrade*, 1993] had both subsequently shown evidence of eddy activity in the Caribbean Sea. Nystuen and Andrade identified two anticyclonic eddies with 20 cm amplitudes and diameters of 200–300 km. These eddies were much larger and more persistent than those previously described, with a comparable westward speed of 15 cm s^{-1}.

In this paper we use sea level information from the TOPEX/POSEIDON satellite altimeters to describe the eddy field in the Caribbean Sea. In addition, an eddy-resolving Atlantic Ocean general circulation model has recently been developed [*Chao et al*., 1996]. The fine horizontal (1/6°) and vertical (37 level) resolution of this simulation allows us to study aspects of the mesoscale dynamics of the Caribbean Sea that are not visible to surface observations from satellite altimetry or drifters.

2. Altimeter Data Analysis

Processing of 110 cycles of TOPEX/POSEIDON (T/P) data (spanning a total of 3 years) into sea level records has been carried out by the Laboratory for Satellite Altimetry, National Oceanographic Data Center, National Oceanic and Atmospheric Administration and is described in detail by *Cheney et al*. [1994]. The along-track resolution is 7 km and the cross-track resolution is 2.83° or 314 km. Orbit precision for the T/P satellite is 5 cm, with most of the error at planetary wavelengths. No filtering has been done to correct for orbit error, as has been necessary with previous altimeter data sets. Ocean tide signals were removed using the tide model of Cartwright and Ray modified by *Wagner et al*. [1994]. The semidiurnal tides are generally weak in the southern Caribbean [*Kjerfve*, 1981], and so errors in the semidiurnal tide correction are not expected to be important.

Sea level variability in the Caribbean rises from a root-mean-square 7 cm in the east to 12 cm in the west, decreasing again as one progresses northward (Figure 4). In the eastern Caribbean, seasonal variations are significant, apparently owing to the annual fluctuations of the trade winds. Between 65°W and 60°W, one fourth of the sea level variability is accounted for by the annual cycle (not shown). We shall see later that eddies grow in amplitude as they propagate through this band of longitudes. The decrease in variability north of the Nicaraguan Rise suggests that many eddies have been dissipated farther south. However, another possibility is that the reduction in variability is due to the limited altimeter data in this region of complex topography. We examine the propagation of the variability within the southern Caribbean by restricting our attention to 14°N, the latitude of maximum observed sea level variability. The results are insensitive to this choice of latitude.

Sea level at a midpoint (14°N, 76.5°W, Figure 5, top) shows strong oscillations at intraseasonal periods throughout the record. To define the timescales of these oscillations, we have computed power spectra using the full record length, without any filtering or prewhitening. The results are displayed in a log linear plot in Figure 5 (bottom). Most of the intraseasonal energy is in the frequency band near 3 months. Examination of spectra as a function of longitude shows that the dominant timescale increases and the frequency band becomes narrower toward the west. At periods of less than 50 days the energy levels drop abruptly.

We examine the temporal variability along 14°N in Plate 1. The longitude-time cross section of sea level at this latitude shows streaks of high sea level associated with a series of 10 distinct anticyclonic eddies and a less distinct number, about 10, of cyclonic eddies propagating westward through the domain. A reexamination of the sea level data from the lower accuracy Geosat altimeter during the 2 years, 1987–1988, has a

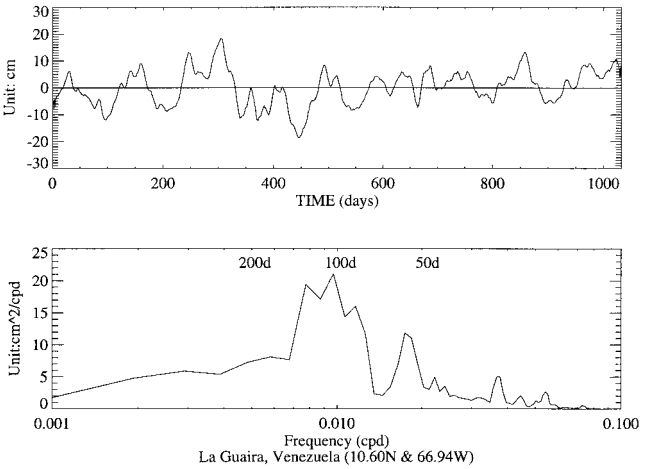

Figure 2. (top) Daily sea level at La Guaira, Venezuela (10.6°N, 66.94°W), for 3 years and (bottom) sea level power spectrum. Data have been daily averaged (data are described by *Muller-Karger and Castro* [1994]).

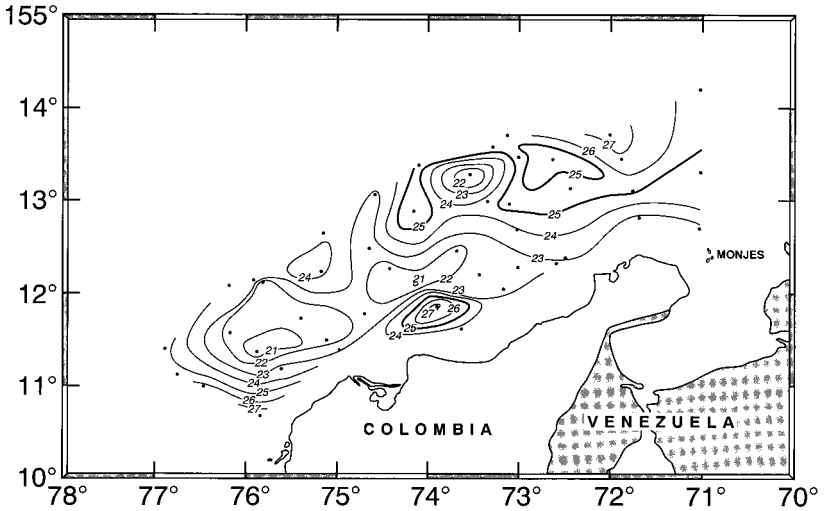

Figure 3. Temperature at 100 m depth based on observations collected by the Colombian Navy between June 24 and July 23, 1975 [*Centro Colombiano de Datos Oceanograficos*, 1983]. During the monthlong cruise the research vessel *San Andres* collected 63 stations, beginning in the west and progressing eastward (indicated by dots). The eddies are spaced approximately 3° apart.

proportionally similar six anticyclonic eddies (not shown). Thus the period of the anticyclonic eddies, 1200/16 ≅ 75 days is consistent with the peak in the sea level spectra presented in Figure 5.

The westward speed of the individual eddies in the TOPEX/POSEIDON data set averaged 11.7 ± 1 cm s^{-1}, which is remarkably consistent with the previous estimates of *Molinari et al*. [1981] and *Nystuen and Andrade* [1993]. We estimate the zonal scale of the eddies to be the distance from the sea level maximum or minimum to the zero crossing after the seasonal cycle is removed. According to this procedure, the average scale of these eddies is 250 km, close to the minimum scale resolvable by the altimeters. It is comforting that the estimate is consistent with that of *Nystuen and Andrade* [1993], although much larger than earlier drifter studies suggested.

The amplitude of the eddies generally grows as the eddies progress westward. In many cases the eddies have substantial amplitude when they first appear in the east Caribbean around 65°W. This observation suggests that many of the eddies have their origin farther east and possibly outside the Caribbean Sea. Because of the large cross-track resolution (314 km) for the T/P data, it is necessary to examine the model simulation discussed below in order to identify the eddies' origin.

3. Analysis of a 1/6° Atlantic Ocean Model Simulation

The ocean model is based on the Parallel Ocean Program (POP) developed at Los Alamos National Laboratory [*Dukowicz et al*., 1993]. This ocean model is based on *Bryan*'s [1969]

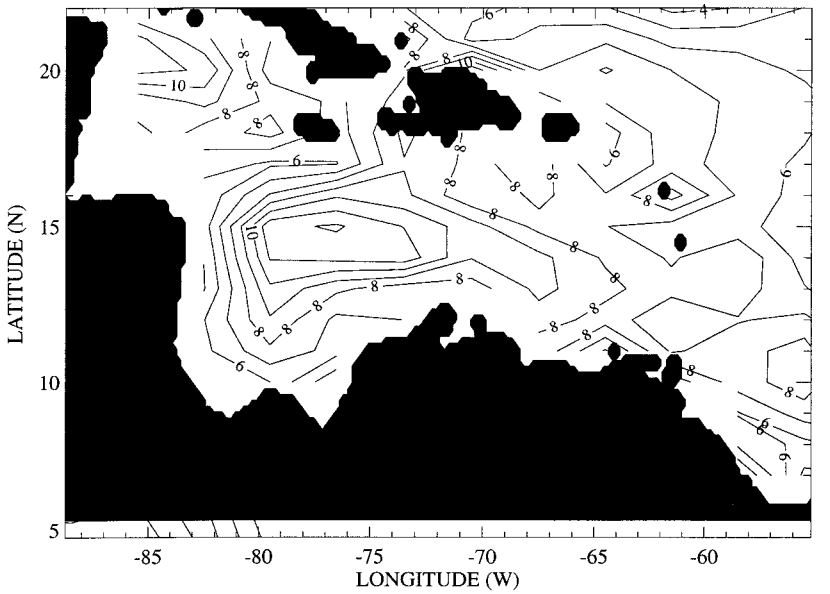

Figure 4. Observed TOPEX/POSEIDON root-mean-square sea surface height. Contour interval is 1 cm.

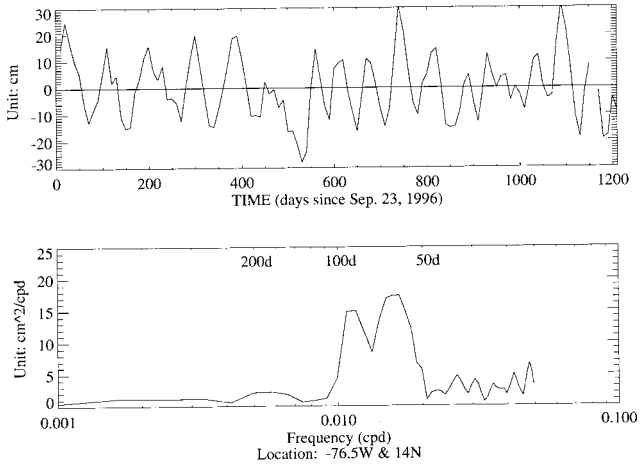

Figure 5. (top) Time series of TOPEX/POSEIDON sea level anomaly at 14°N, 76.5°W and (bottom) sea level power spectrum.

formulation but differs from it by removing the rigid-lid approximation and treating the sea surface height as a prognostic variable (i.e., free surface). The model domain covers the Atlantic Ocean from 35°S to 80°N. The horizontal resolution is 1/6° in both longitude and latitude. There are 37 levels in the vertical. For the horizontal subgrid-scale parameterization of tracers and momentum, a highly scale-selective biharmonic (fourth order) scheme was used. The conventional second-order operator is used for the vertical subgrid-scale parameterization. The ocean model is closed to inflow and outflow at the open boundaries. To mimic the water exchange processes across these artificial boundaries, "sponge" layers (or "buffer" zones) are introduced next to these closed boundaries at all depths. In these sponge layers, temperature and salinity are restored toward the *Levitus* [1982] seasonal climatology. The width of the sponge layer is about 5°, and the restoring timescale decreases from 30 days for grid points near the prognostic model interior to 5 days near the boundary.

Starting from *Levitus* [1982] initial conditions, we have integrated this 1/6° Atlantic Ocean model for a total of 30 years. During the first 10 years the model was forced with climatological wind stress of *Hellerman and Rosenstein* [1983] and heat flux of *Han* [1984]. Surface salinity was restored to the *Levitus* [1982] climatology with a timescale of 30 days. During the last 20 years the model was forced with European Centre for Medium-Range Weather Forecasts (ECMWF) monthly stresses [*Trenberth and Olson*, 1988; *Barnier et al*., 1995]. The last 1200 days of the model simulation have been used in the current analysis, starting from day 6717. Preliminary results evaluating model performance are presented by *Chao et al*. [1996].

The distribution of simulated sea level variability (Figure 6) bears similarities to that observed by TOPEX/POSEIDON (Figure 4), with maximum variability in the west and a band of enhanced variability extending eastward at roughly 14°N. Much of the difference in amplitude between sea level variability as observed by TOPEX/POSEIDON and that produced by the numerical model may result from limitations of the spatial resolution of TOPEX/POSEIDON observations. When the TOPEX/POSEIDON observations are compared with ERS 1 observations with 4 times the spatial resolution (and a 35-day repeat orbit), the positions of the eddies are the same but the eddy amplitudes increase by a factor of 2 (Figure 7). The short year and a half length of the 35-day repeat ERS 1 record precludes its use in a statistical comparison to the simulation.

The distribution of simulated sea level power also bears strong similarities to the TOPEX/POSEIDON observations as a function of frequency, but with increased amplitude (compare Figures 5 and 8). The sea level spectrum at 76.6°W reaches a peak of 37 cm^2 cpd^{-1} at approximately 80 days (0.013 cpd). Energy in periods less than 50 days (0.02 cpd) is greatly reduced.

In addition to having enhanced variability overall, the simulation has its strongest variability in the Gulf of Mexico,

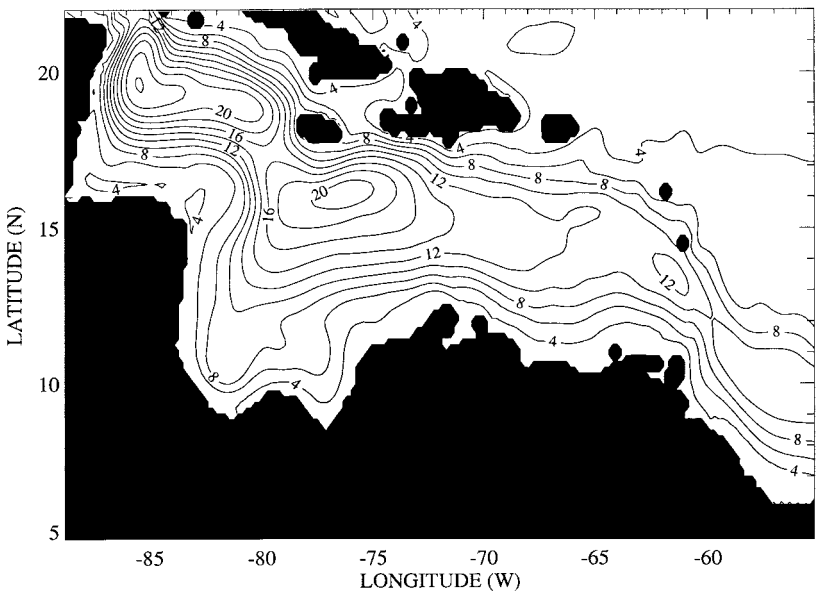

Figure 6. Simulated root-mean-square sea level from 1/6° Atlantic ocean general circulation model. Contour interval is 2 cm.

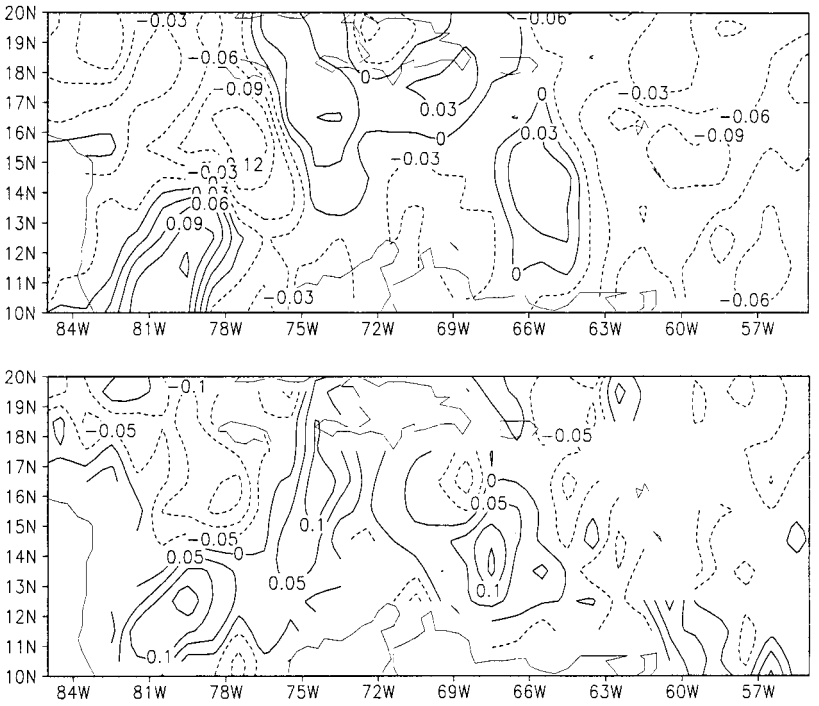

Figure 7. Sea level anomaly in mid-January 1993 as observed by (top) TOPEX/POSEIDON and (bottom) ERS 1.

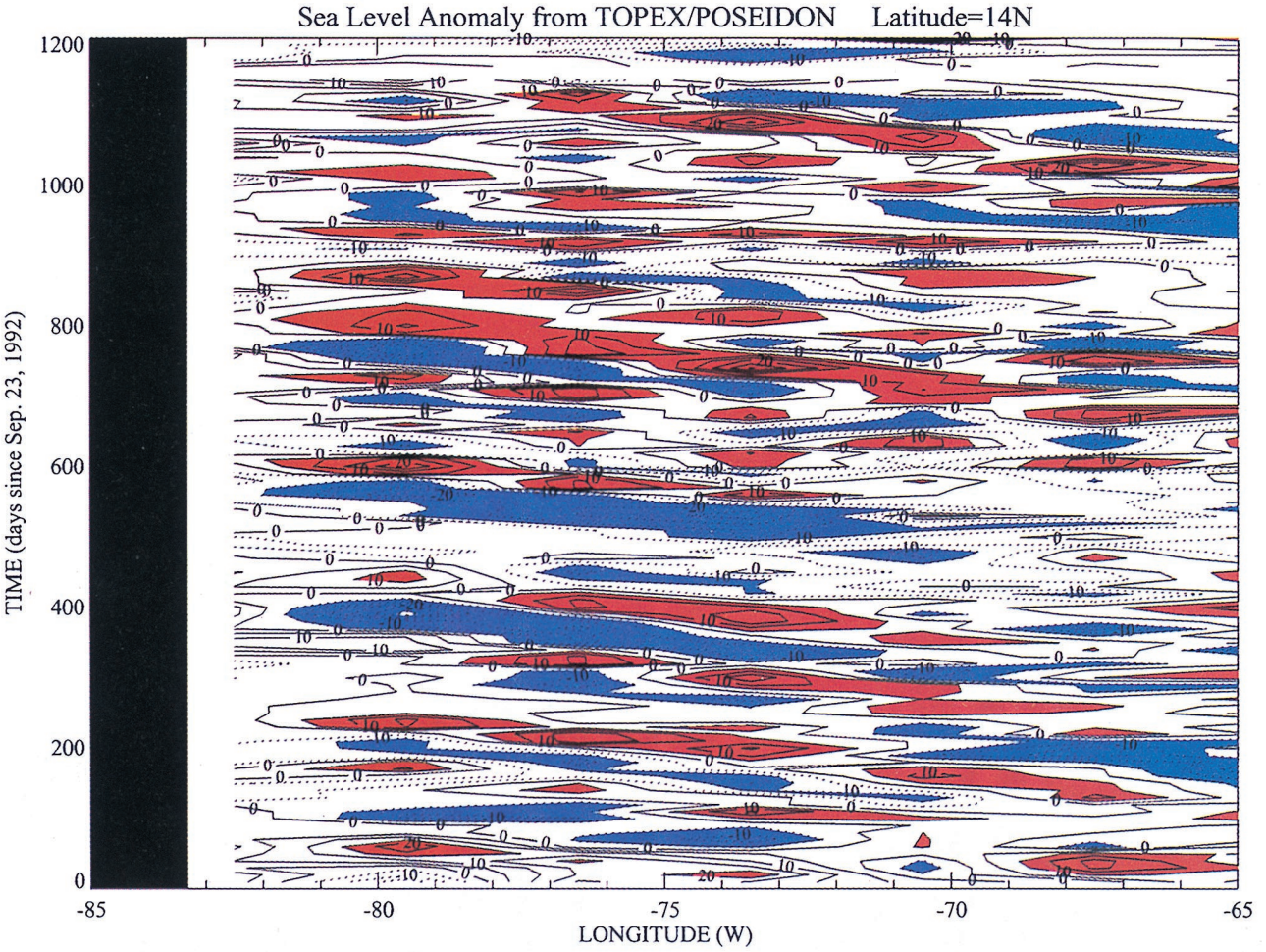

Plate 1. Cross section of observed sea level with longitude and time at 14°N. Contour interval is 5 cm. Anomalies exceeding 10 cm are shaded.

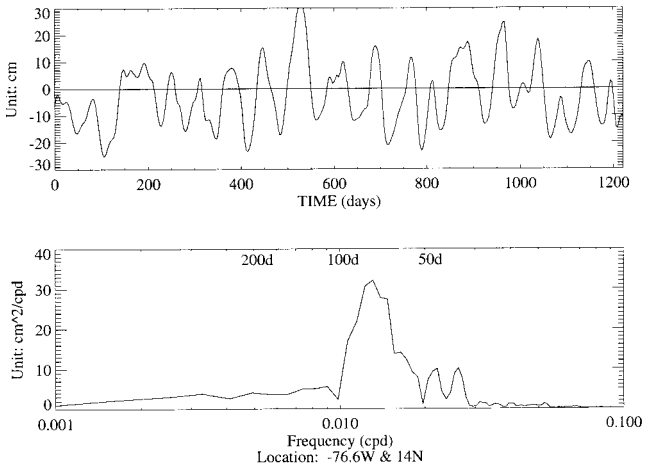

Figure 8. Simulated sea level at 14°N, 76.5°W, (top) time series and (bottom) power spectrum. Simulated sea level variability is somewhat higher than observed (compare with Figure 5).

rather than the southern Caribbean. It appears that a large fraction of the eddies in the simulation are able to travel past the Yucatan peninsula, contributing to the variability of the Gulf of Mexico. Visual inspection of the TOPEX/POSEIDON record suggests that a majority of the observed eddies spin down in the western Caribbean, near the coast of Nicaragua, before passing the Yucatan peninsula.

Clearly, most of the simulated variability in the 50- to 100-day (0.01–0.02 cpd) band is also the result of westward eddy propagation (compare Plates 1 and 2). East of the Caribbean (not shown), sea level variations are primarily annual; but, within the Caribbean the sea level field is even more strongly dominated by westward propagating eddies than observed. The average propagation speed, 12 cm s^{-1}, and spatial scales, typically 200–300 km, are similar to those observed.

An instantaneous cross section of temperature, salinity, and velocity with depth and longitude along 14°N (Figure 9) shows a distinct cyclonic eddy at 70°W. Consistent with the observations of *Morrison and Nowlin* [1982], the eddy is confined to the thermocline (upper 200 m), with little vertical phase shift. A second cyclonic eddy appears near the coast of Nicaragua at 80°W and penetrates much more deeply into the water column to 600 m.

If one assumes that the eddies conserve mass and potential vorticity as they shift westward, then the vertical stretching the eddies experience would result in an increase in the amplitude of the sea level anomaly and a corresponding decrease in horizontal scale. An alternative explanation for the observed doubling of amplitude of the eddies is growth by instability. Strong vertical as well as horizontal shears are present in this

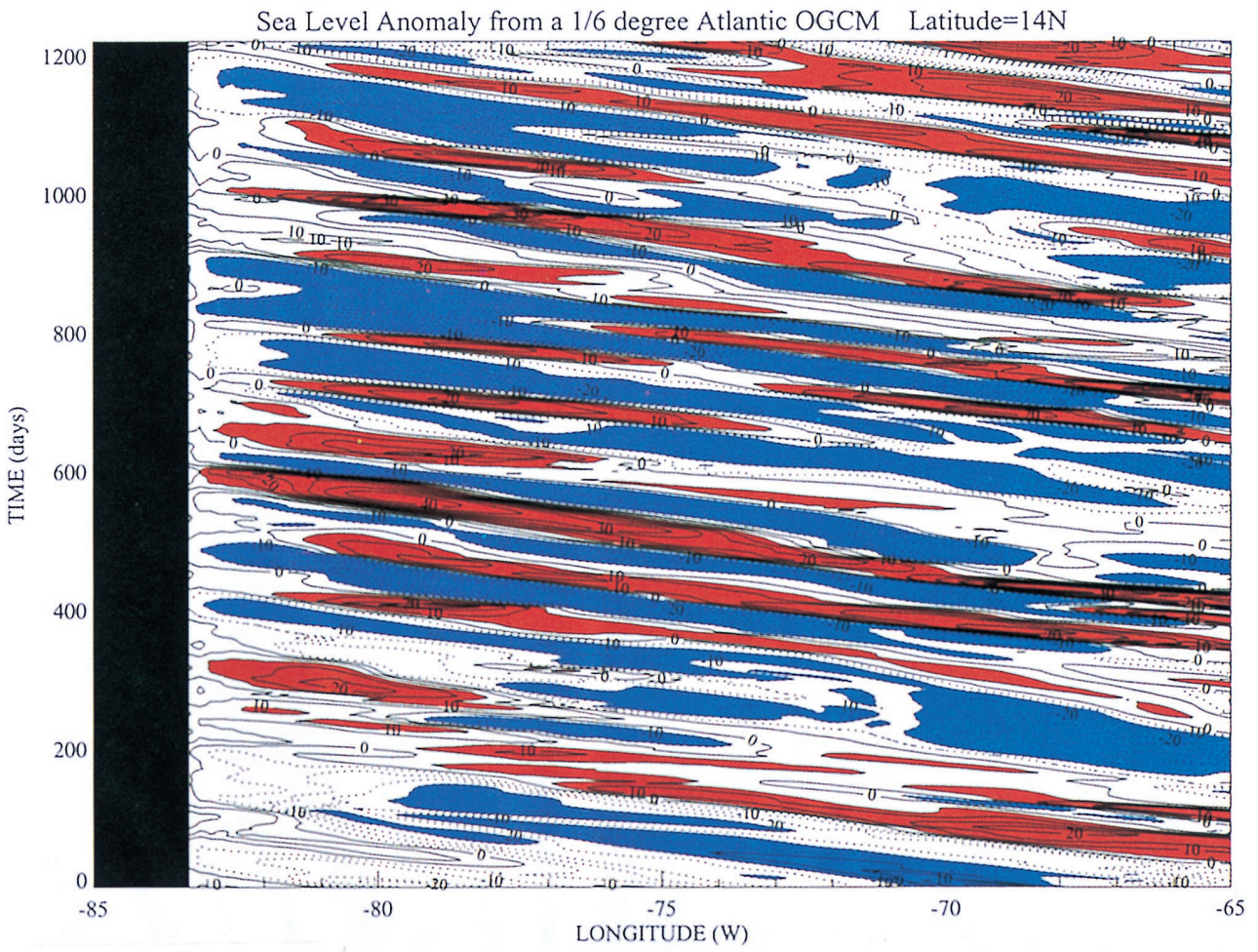

Plate 2. Cross section of simulated sea level with longitude and time at 14°N. Contour interval is 5 cm. Anomalies exceeding 10 cm are shaded.

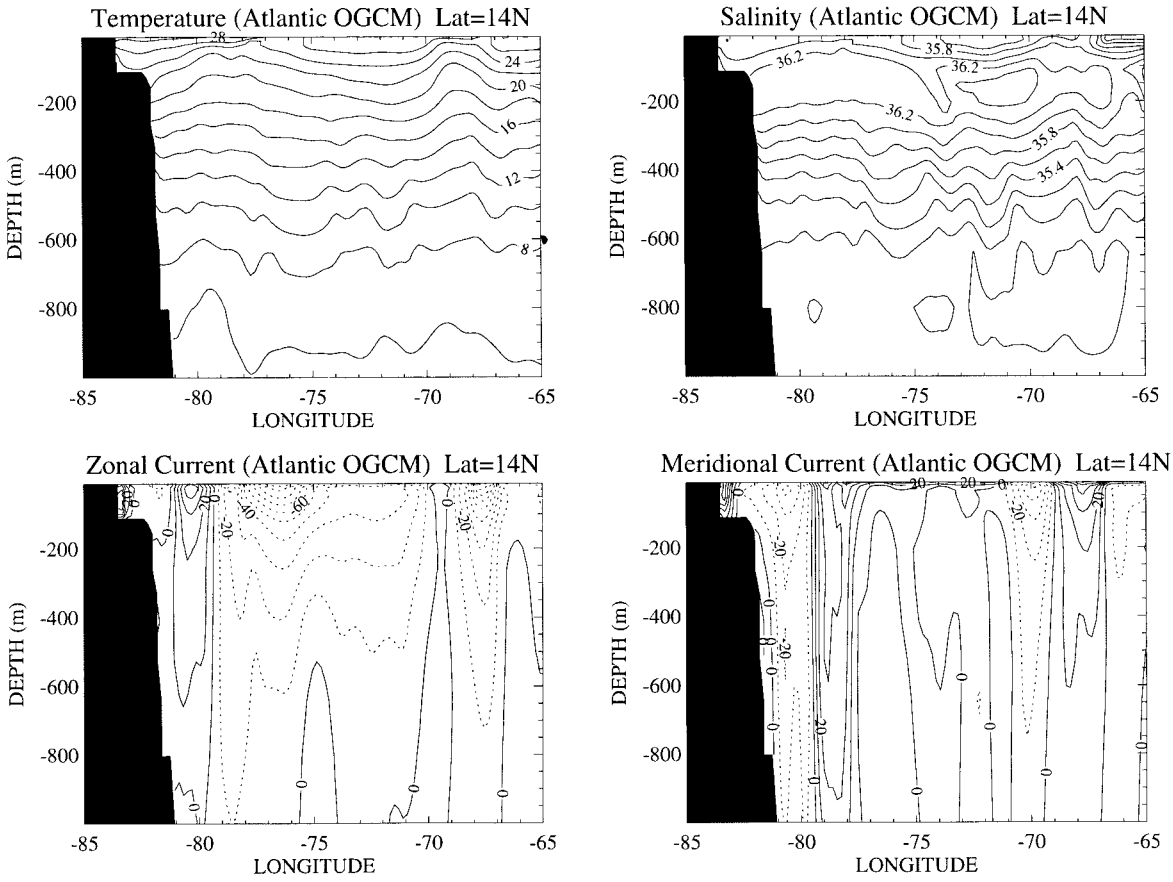

Figure 9. Vertical structure of simulated temperature, salinity, and velocity at 14°N on day 6780.

region. Simple application of necessary conditions for instability growth suggests that either barotropic- or baroclinic-type instabilities may be important.

4. Life Cycle of Two Anticyclonic Eddies

The life cycle of several anticyclonic eddies is shown in Plate 3 (sea level) and Figure 10 (surface current). We begin soon after the first eddy has been formed in the retroflection of the North Brazil Current (day 7371, Plate 3, top left). After formation this ring-like eddy progresses to the northwest at a speed of 15 cm s^{-1} on day 7401. Figure 10a shows this eddy with its western edge at the longitude of the Lesser Antilles on day 7401. By 7431 the eddy has become elongated and has partially crossed the line of islands, and by 7461 it has fully entered the southern Caribbean. In Figure 10b we follow a second anticyclonic eddy that is adjacent to the Lesser Antilles on day 7551. This eddy clearly induces a cyclonic circulation to its west. By day 7611 both the original anticyclonic eddy and the cyclonic eddy to its west have entered the Caribbean Sea. This cyclone-anticyclone pair progresses westward through the southern Caribbean during an interval of 170 days. In the simulation these eddies are dissipated farther north along the Yucatan peninsula.

The simulated eddy shedding near the North Brazil retroflection is consistent with recent field observations of *Johns et al*. [1990] and *Fratantoni et al*. [1995] showing that the currents along the northeastern margin of Brazil are quasi-periodic with periods between 40 and 100 days. On the basis of these observations and images from the coastal zone color scanner, Johns et al. suggest that the North Brazil retroflection system is unstable, continuously shedding anticyclonic rings. Inspired by this work, *Richardson et al*. [1994] report surface drifter tracks that show two such rings progressing northwestward to the Lesser Antilles. At that point the rings either spun down or ejected the drifters. Using the Geosat altimeter data, *Didden and Schott* [1993] trace retroflection rings as far as the entrance to the Caribbean Sea, leaving their fate farther downstream uncertain.

Fratantoni et al. [1995] revisit the issue of the fate of the rings. They examine a numerical simulation of the tropical Atlantic using a 1/4° × 1/4°, six-layer model. Examination of the model output shows that although rings form every 40–60 days, only three to four rings per year can be traced to the Lesser Antilles, and none penetrates into the Caribbean. However, in evaluating their model, one must consider the complex geometry of the Lesser Antilles. The coastline for that particular model was defined by the 200-m isobath. That approximation and the 1/4° × 1/4° resolution effectively close most of the southern passages into the Caribbean in that model (the complexity of the topography is described by *Mazeika et al*. [1983] and *Kinder et al*. [1985]). Recent results with an extremely high resolution 1/12° × 1/12° version of the Miami Isopycnic Coordinate Model as well as a 1/10° × 1/10° resolution run using the POP model shows an eddy field evolving in many ways similar to the results presented here (E. Chassignet,

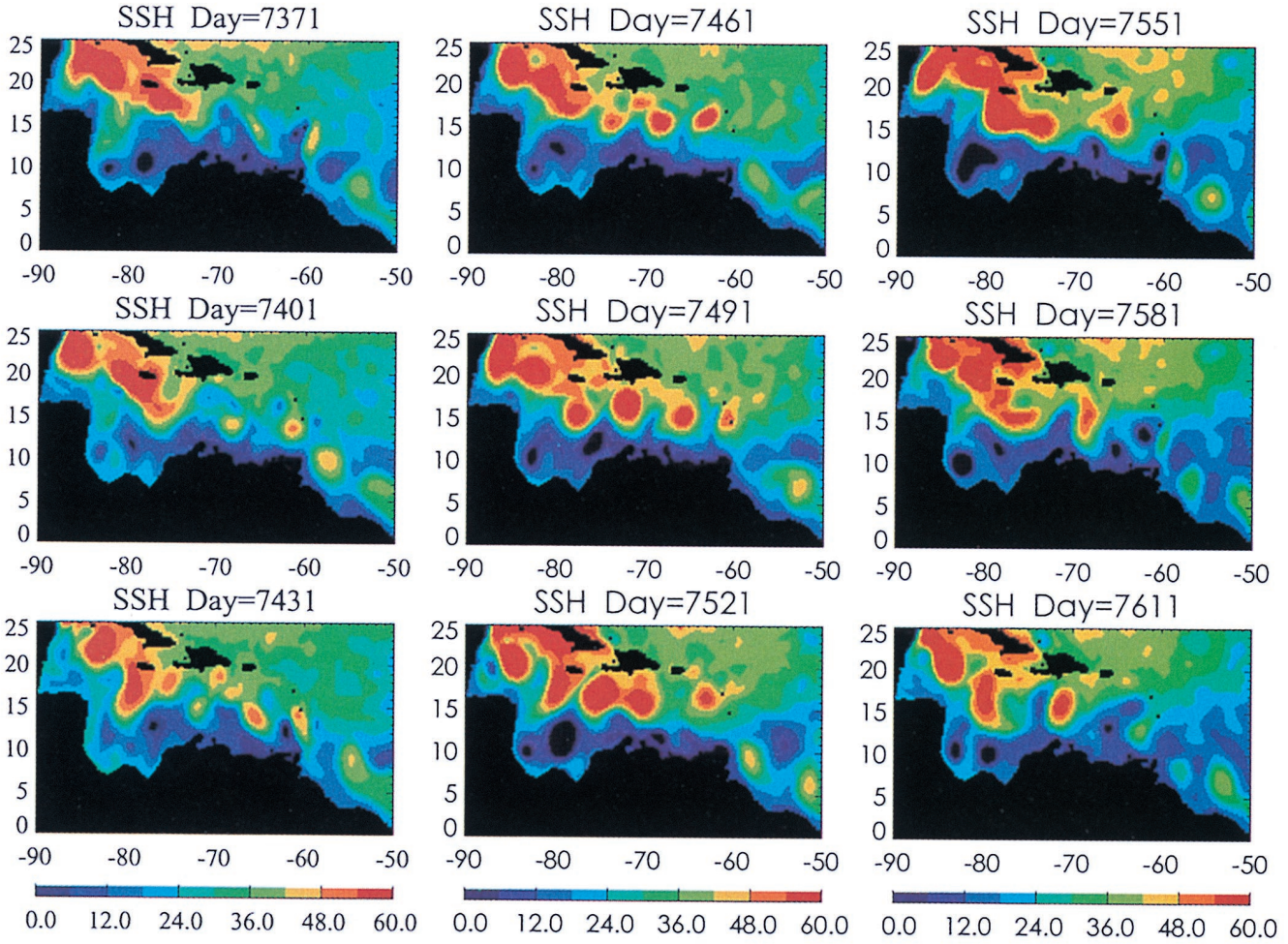

Plate 3. Simulated sea level height at 30-day intervals from days 7371 to 7611. Note the penetration of several anticyclonic eddies into the Caribbean Sea.

personal communication, 1998; R. Smith, personal communication, 1998).

5. Summary

The Caribbean Current is the major route by which water enters the Gulf of Mexico, likely an important carrier of Southern Hemisphere water, and thus is an important upper branch of the North Atlantic circulation system. Historical hydrographic, sea level, and drifter data have long suggested the presence of strong eddies in this region. These eddies may potentially be playing an important role in the North Atlantic circulation by exchanging Caribbean Current mass and momentum with the surrounding waters. In this paper we use sea level observations from the first 3 years of the TOPEX/POSEIDON altimeter mission to show the presence of large, regular, cyclonic, and anticyclonic eddies throughout the southern basin.

The presence of these eddies raises questions about their origin, ultimate fate, and relationship to the mean circulation of the Caribbean. To begin to address these questions, we turn to a numerical model simulation, part of an eddy-resolving simulation of Atlantic circulation. Our conclusions can be summarized as follows:

1. The Caribbean supports strong eddy activity with near 3-month timescales and 250-km spatial scales. The eddies progress westward with speeds of 12 cm s^{-1}, taking approximately 180 days to cross the basin before dissipating near the coast of Nicaragua or the Yucatan peninsula. The speeds are similar to those of freely propagating waves, but their growth in amplitude westward and changing vertical structure (in the model simulation) suggest that a combination of vortex stretching and sheer instability effects may be important as well.

2. An eddy-resolving general circulation model of the tropical and North Atlantic has been developed and is found to reproduce these eddies. The simulation results strongly suggest that the eddies ultimately originate in the formation of anticyclonic rings in the North Brazil retroflection. It has been well documented that the North Brazil Current retroflection produces anticyclonic eddies at a rate of two to three per year. These have been traced previously northwestward toward Port of Spain at the entrance to the southern Caribbean. The simulation presented here provides an extra chapter to this story. The simulation shows the eddies interacting with the topography associated with the islands of Trinidad and Tobago. The interaction produces a cyclonic circulation to the west of each ring. The resulting pairs of cyclonic and anticyclonic eddies become part of, and interact with, the Caribbean Current. In the simulation many of the anticyclonic eddies sweep westward past the Yucatan peninsula before finally decaying in the Gulf of Mexico.

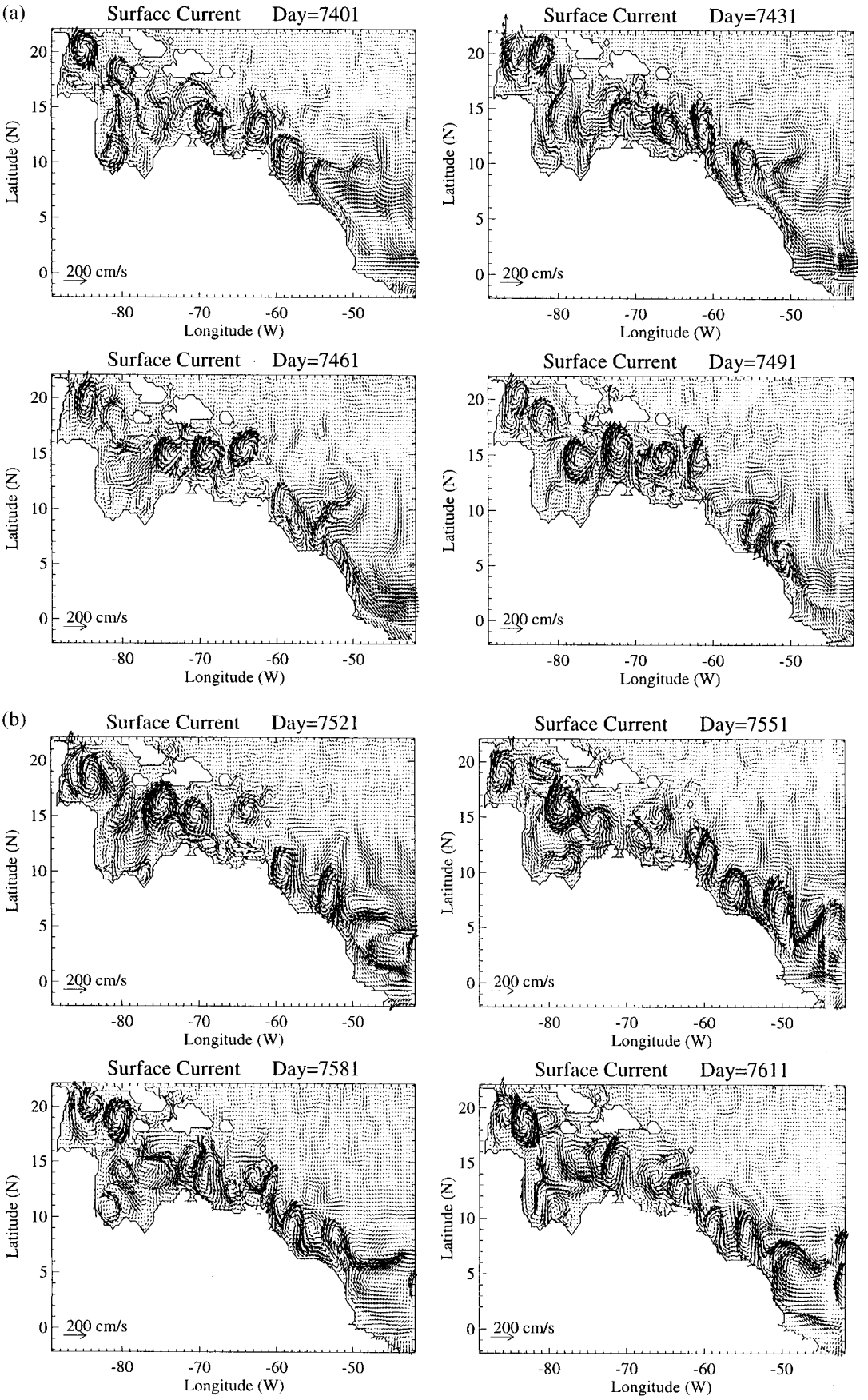

Figure 10. Simulated surface currents for two 90-day intervals, (a) 7401–7491 and (b) 7521–7611. Anticyclonic eddies are apparent at the entrance to the Caribbean Sea on days 7431 and 7551. The subsequent maps show the penetration of these eddies westward.

Our hypothesis of the generating mechanism of the Caribbean Sea eddies must be treated as tentative. It would be interesting to compare our 1/6° model simulation with other model simulations at higher spatial resolution (1/10° and 1/12°). Further sensitivity experiments are required to confirm our eddy generation hypothesis.

Acknowledgments. The authors thank F. Muller-Karger for providing the sea level time series at La Guaira, Venezuela, and R. E. Cheney and the Laboratory for Satellite Altimetry/NODC/NOAA for providing the altimetry. The numerical simulation described in this publication was carried out by Y.C. at the Jet Propulsion Laboratory (JPL), California Institute of Technology, under a contract with National Aeronautics and Space Administration. Computations were performed on the 256-processor Cray T3D massively parallel computer through the JPL Supercomputing Project. J.A.C. has been supported by the National Science Foundation under grant OCE9416894.

References

Barnier, B., L. Siefridt, and P. Marchesiello, Thermal forcing for a global ocean circulation model from a three-year climatology of ECMWF analysis, *J. Mar. Syst*., *6*, 363–380, 1995.

Bryan, K., A numerical method for the study of the circulation of the world ocean, *J. Comput. Phys*., *4*, 1687–1712, 1969.

Centro Colombiano de Datos Oceanograficos, *Crucero Oceano IV - Areas 2 and 3*, 8 pp., 9 tables, 43 figures, Repub. de Colombia Armada Nac., Bogota, 1983.

Chao, Y., A. Gangopadhyay, F. Bryan, and W. R. Holland, Modeling the Gulf Stream System: How far from reality?, *Geophys. Res. Lett*., *23*, 3155–3158, 1996.

Cheney, R., L. Miller, R. Agreen, N. Doyle, and J. Lillibridge, TOPEX/POSEIDON: The 2-cm solution, *J. Geophys. Res*., *99*, 1150–1165, 1994.

Didden, N., and F. Schott, Eddies in the North Brazil Current retroflection region observed by Geosat altimetry, *J. Geophys. Res*., *98*, 20,121–20,131, 1993.

Dukowicz, J. K., R. D. Smith, and R. C. Malone, A reformulation and implementation of the Bryan-Cox-Semtner ocean model on the connection machine, *J. Atmos. Oceanic Technol*., *10*, 195–208, 1993.

Fratantoni, D. M., W. E. Johns, and T. L. Townsend, Rings of the North Brazil Current: Their structure and behavior inferred from observations and a numerical simulation, *J. Geophys. Res*., *100*, 10,633–10,654, 1995.

Fu, L. L., and B. Holt, Some examples of oceanic mesoscale eddies by the Seasat synthetic aperture radar, *J. Geophys. Res*., *88*, 1844–1852, 1983.

Gordon, A. L., Circulation in the Caribbean Sea, *J. Geophys. Res*., *72*, 6207–6223, 1967.

Han, Y. J., A numerical world ocean General Circulation Model, II, A baroclinic experiment, *Dyn. Atmos. Ocean*, *8*, 141–172, 1984.

Heburn, G. W., T. H. Kinder, J. H. Allender, and H. E. Hurlburt, A numerical model of eddy generation in the southeastern Caribbean Sea, in *Hydrodynamics of Semi-enclosed Seas*, edited by J. C. J. Nihoul, pp. 299–328, Elsevier, New York, 1982.

Hellerman, S., and M. J. Rosenstein, Normal monthly wind stress over the world ocean with error estimates, *J. Phys. Oceanogr*., *13*, 1093–1104, 1983.

Ingham, M. C., and C. V. W. Mahnken, Turbulence and productivity near St. Vincent Island, B.W.I., A preliminary report, *Caribbean J. Sci*., *6*, 83–87, 1966.

Johns, W. E., T. N. Lee, and F. A. Schott, The North Brazil Current retroflection: Seasonal structure and eddy variability, *J. Geophys. Res*., *95*, 22,103–22,120, 1990.

Kinder, T., Shallow currents in the Caribbean Sea and Gulf of Mexico as observed with satellite-tracked drifters, *Bull. Mar. Sci*., *33*, 239–246, 1983.

Kinder, T. H., G. W. Heburn, and A. W. Green, Some aspects of the Caribbean circulation, *Mar. Geol*., *68*, 25–52, 1985.

Kjerfve, B., Tides in the Caribbean Sea, *J. Geophys. Res*., *86*, 4243–4247, 1981.

Leming, T. D., Eddies west of the southern Lesser Antilles, in *Symposium on Investigations and Resources of the Caribbean Sea and Adjacent Regions*, pp. 113–120, UNESCO, Paris, 1971.

Levitus, S., *Climatological atlas of the world ocean*, *NOAA Prof. Pap. 13*, 174 pp., U.S. Govt. Print. Off., Washington, D. C., 1982.

Mazeika, P. A., T. H. Kinder, and D. A. Burns, Measurements of subtidal flow in the Lesser Antilles passages, *J. Geophys. Res*., *88*, 4483–4488, 1983.

Molinari, R. L., M. Spillane, I. Brooks, D. Atwood, and C. Duckett, Surface currents in the Caribbean Sea as deduced from Lagrangian observations, *J. Geophys. Res*., *86*, 6537–6542, 1981.

Morrison, J. M., and W. D. Nowlin Jr., General distributions of water masses within the eastern Caribbean Sea during the winter of 1972 and the fall of 1983, *J. Geophys. Res*., *87*, 4207–4229, 1982.

Muller-Karger, F. E., and R. A. Castro, Mesoscale processes affecting phytoplankton abundance in the southern Caribbean Sea, *Cont. Shelf Res*., *14*, 199–221, 1994.

Nystuen, J. A., and C. A. Andrade, Tracking mesoscale ocean features in the Caribbean Sea using Geosat altimetry, *J. Geophys. Res*., *98*, 8389–8394, 1993.

Richardson, P. L., G. E. Hufford, R. Limeburner, and W. S. Brown, North Brazil current eddies, *J. Geophys. Res*., *99*, 5081–5093, 1994.

Schmitz, W. J., Jr., and P. L. Richardson, On the sources of the Florida Current, *Deep Sea Res*., *Part B*, *B38*, suppl. 1, S379–S409, 1991.

Trenberth, K. E., and J. G. Olson, ECMWF global analysis 1979–86: Circulation statistics and data evaluation, *Tech. Note NCAR/TN-300+STR*, 94 pp., 12 fiche, Natl. Cent. for Atmos. Res., Boulder, Colo., 1988.

Wagner, C. A., C. K. Tai, and J. M. Kuhn, Improved M_2 ocean tide from TOPEX/POSEIDON and Geosat altimetry, *J. Geophys. Res*., *99*, 24,853–24,866, 1994.

Wust, G., *Stratification and Circulation in the Antillean-Caribbean Basin*, 201 pp., Columbia Univ. Press, New York, 1964.

J. A. Carton, Department of Meteorology, University of Maryland at College Park, 3433 Computer and Space Science Building, College Park, MD 20743. (carton@atmos.umd.edu)

Y. Chao, Jet Propulsion Laboratory, California Institute of Technology, Pasadena, CA 91109. (yc@pacific.jpl.nasa.gov)

(Received April 16, 1998; revised October 22, 1998;
accepted November 20, 1998.)